



Monitoring network design with MLPG-TLBO hybrid model (case study Birjand, Iran)

Nahid Majidi Khalilabad¹ · Ali Mohtashami² · Mahdi Khorashadizadeh² · Abolfazl Akbarpour³

Received: 17 August 2021 / Accepted: 8 March 2022 / Published online: 15 April 2022
© The Author(s) 2022

Abstract

As the groundwater quantitative monitoring aimed to determine the factors affecting the aquifer behavior plays an important role in its regional management, studying the temporal and spatial groundwater level variations requires a comprehensive monitoring network. Effort has been made in this study to introduce a new linked simulation–optimization method, named MLPG-TLBO to quantitatively monitor the Birjand aquifer and determine the optimal points for piezometers. This model uses meshless local Petrov Galerkin (MLPG) method in the simulation part and teaching–learning-based optimization (TLBO) method in the optimization part. The objective function, in this study, is to minimize the difference between the groundwater level observed in piezometers and obtained computationally by the model. Since this coupled model is independent from the meshing, it eliminates the mesh-dependent shortcomings and, hence, yields more accurate results. It has been calibrated and validated in previous Birjand area studies and has led to acceptable results. By implementing the model in Birjand aquifer, the optimal positions of ten piezometers were determined mostly in areas where the density of the extraction wells was lower. Finally, the RMSE of both MLPG-TLBO and FDM was obtained to be 0.334 m and 1.483 m for 10 optimal piezometers. The RMSE value for MLPG-TLBO has shown a 0.423 m reduction compared to its previous value. This difference is quite meaningful as it shows good performance of this method in designing an optimal network for the aquifer.

Keywords Monitoring network · MLPG simulation model · TLBO algorithm · Birjand aquifer

Introduction

The hydrometric monitoring network plays an important role in the planning and management of water resources and its design for the groundwater aquifer can either be qualitative or quantitative, but this does not mean that they do not do each other's duty; it rather shows that their design methods change according to the users' objectives. Therefore, in a monitoring network proportionate to the aquifer conditions, the concepts of protection and maintenance, as well as the development and updating to receive highly uncertain

hydrometric information, will be very important (Mishara and Coulibaly 2009).

The hydrogeological modeling methods of the groundwater monitoring are either statistical or probabilistic, both of which require the access to sufficient information on the quantitative and qualitative status of the aquifer for optimal management (Mohtashami et al. 2017). The groundwater level study/evaluation through the existing models facilitates the behavior prediction of groundwater resources. Since the groundwater monitoring network design is an optimization issue requiring high computation costs, it should provide the best results with the least number of observation wells.

Studies on the quantitative and qualitative design of the aquifer monitoring network are numerous. Using the genetic algorithm, Cieniawski et al. (1995) determined the location of groundwater monitoring wells to examine such objectives as the maximum reliability and minimum contaminated areas in the initial diagnoses. They considered 162 monitoring-well positions, evaluated the Pareto front values for 4 and 5, and showed that the reliability was 48–90% and contamination was 3.5–14.5 hectares based on the

✉ Abolfazl Akbarpour
akbarpour@birjand.ac.ir

¹ Research Assistant of East Water and Environmental Research Institute (EWERI), Mashhad, Iran

² Department of Civil Engineering, University of Sistan and Baluchestan, Zahedan, Iran

³ Department of Civil Engineering, University of Birjand, Birjand, Iran

considered conditions and results (Cieniawski et al. 1995). In a study performed in the California National Laboratory for groundwater quality monitoring, Kollat et al. (2011) used the NSGAI algorithm aimed to reduce the contaminant concentration estimation errors, contamination load estimation errors and costs caused by the leakage of the PCE contaminant from an underground tank (Kollat et al. 2011). There were 29 wells in the flow path, and the Pareto front was obtained for 18 to 25 monitoring wells. They showed that the algorithm was able, in all the considered cases, to provide different options for the location of monitoring wells in accordance with the objective functions. To optimally design the groundwater quality monitoring network and show spatiotemporal densities, Dhar and Patil (2012) used the non-dominated sorting multi-objective genetic optimization algorithm and the conventional fuzzy Kriging method to determine the minimum number of piezometric wells in a real Aquifer of India (Dhar and Patil 2012). Aboutalebi et al. (2017) used the NSGAI algorithm for the optimal design of monitoring networks in river-reservoir systems and minimized the average contaminant detection time and concentration prediction error at sampling stations using the multi-objective optimization method (Aboutalebi et al. 2017). Aiming at reducing the number of piezometers without affecting the data quality and using KGA (Kriging-combined genetic algorithm) and PSO (particle swarm optimization) algorithms, Khorramdel and Kekhaei (2016) studied the Astaneh-Kuchesfahan aquifer in the north of Iran to optimize the monitoring network. They showed, through the results, that the number of observation wells in this aquifer could reduce by 26% without any losses in the data quality (Khorramdel and Kekhaei 2016). Aiming at minimizing the number of piezometric wells and estimation error, Mirzaei Nodooshan et al. (2016) used the NSGAI algorithm to locate piezometric wells and introduced 311 points in Eshtehard aquifer to the NSGAI algorithm as potential points for which the observational groundwater levels were interpolated using real piezometers and interpolation tools in the GIS environment. Locating was done by the NSGAI algorithm and the decision variable was the piezometric wells (Mirzaei Nodooshan et al. 2016). Mirzaei Nodooshan et al. (2019) presented an optimization-based method for the network design of the groundwater level monitoring and used it for the Eshteharud plain aquifer. Scenarios they considered to optimize the position of observational wells were: (1) Selecting optimum number of wells from among those in the study area and (2) Adding optimum number of monitoring wells to the existing ones. Results showed that their method could omit a number of extra wells in an existing monitoring network with acceptable accuracy or add some if it lacked any (Mirzaei Nodooshan et al. 2019). To monitor the Gilan plain aquifer qualitatively, Janatrostami and Salahi (2020) used the GA optimization method

and showed that it was acceptable based on the calculated error criteria. Since the spatial distribution studies and comparison of the average observed regional salinity with that calculated in the optimal network (covering all selected monitoring wells) showed that the calculated values were larger than the observed average, the network provided the optimal data of the groundwater quality in more polluted areas (Janatrostami and Salahi 2020). Temur (2021) used the hybrid TLBO algorithm for Optimum design of cantilever retaining walls under seismic loads. The robust results were obtained by HTLBO with 50 populations. Consequently, the results showed that the hybrid TLBO algorithm optimized the implementation cost of RC cantilever retaining walls well (Temur 2021). Recently, various researchers have used combined optimization algorithms to overcome computational complexity. Veladi and Beig Zali (2021), to optimally design single-layer dome structures, used the hybrid TLBO algorithm. The analysis results during this comparative process indicate that the hybrid TLBO algorithm provides a better and simpler design in less time than the standard algorithms (Veladi and Beig Zali 2021).

A literature review reveals that research that combines numerical and optimization models to design a monitoring network is rare. Numerical models simulate the desired phenomenon with great accuracy and predict and simulate its behavior through the provided input information (Khorashadzadeh et al. 2020). Those used in the groundwater domain are summarized in the finite difference and finite element methods, which form the basis for GMS and FEFLOW, respectively (Majidi Khalilabad et al. 2021). Use is recently made, in this domain, of new meshless numerical methods that can be improved by the user-required possibilities besides being more accurate and capable than their predecessors due to their being open-source (Liu and Gu 2001). Meshless methods have a wide range including the “smoothed-particle hydrodynamics (SPH),” “element-free Galerkin (EFG),” “meshless local Petrov–Galerkin (MLPG),” and so on. As choosing a method depends on its application, it is better to use specific methods in fluid-related problems.

The aim of this study is to use a numerical and an optimization model together to design a monitoring network optimally. The MLPG numerical method and the TLBO (training-learning-based optimization) algorithm were linked together recognized as simulation and optimization models to develop a simulation–optimization model for the design of an optimal monitoring network on Birjand aquifer in South Khorasan province.

Materials and methods

Case study

Birjand aquifer, in South Khorasan province, is 269 km² in area containing 190 extraction wells and 10 piezometric wells. It is 1491 m above the sea level with an annual rainfall of 160 mm and is known as a dry-climate region according to the Domarton classification. Figure 1 shows the location

of the aquifer, extraction wells (blue) and piezometric wells (red) (Khorashadizadeh et al. 2016 and 2018).

Teaching-learning-based optimization method

Rao et al. (2011) were the first to introduce the TLBO algorithm in the “Computer-Aided Design” Journal to solve the related problems (Rao et al. 2011), but about a year later, they introduced it in the “Information Sciences” Journal in a larger scale and for more general problems (Rao et al. 2012).

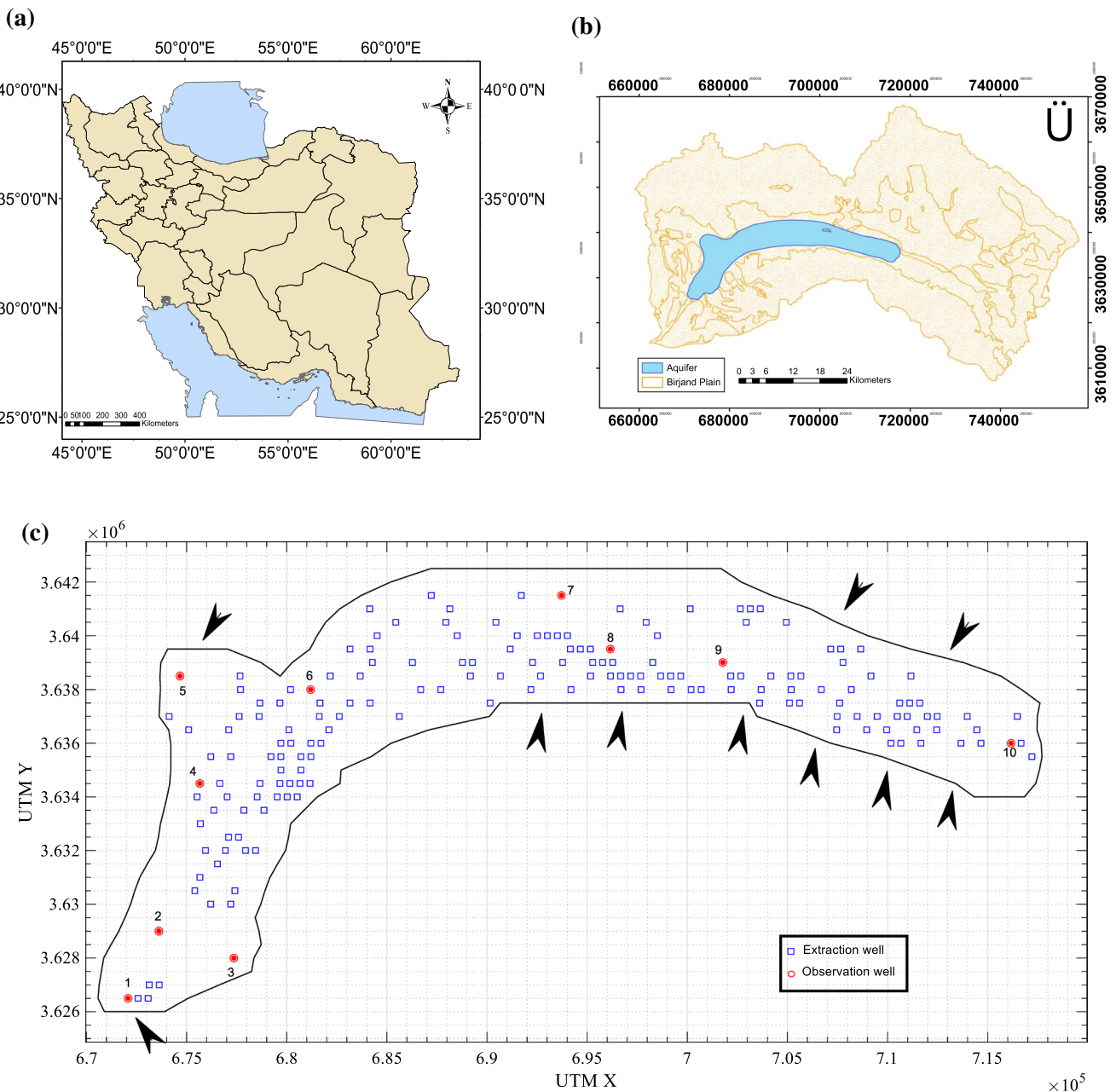


Fig. 1 Location of Birjand unconfined aquifer in Iran (Mohtashami et al. 2022)

Contrary to other meta-heuristic methods that usually model the nature, the TLBO algorithm (described later in more details) models the classroom teacher-student process and uses it to find the optimal solution. It is based on teaching (teacher) and learning (student) steps and its output at each step is the students' scores and level of knowledge (Črepinšek et al. 2012).

Generation of initial population

In the first step, a series of points (students) are formed and distributed randomly in the solution space and then, the objective function (students grades and level of knowledge) is calculated for each point based on the problem's main objective function and coordinates of each point; the score distribution has been assumed to be bell-shaped (Fig. 2) without reducing the problem all-inclusiveness. As shown, the best student becomes the teacher and the training step begins.

Teaching stage

Here, the point specified the "best" by the objective function becomes the teacher and starts teaching others; in other words, all the points with situations worse than the teacher move toward the latter causing the average distribution to move toward it. It is worth noting that in meta-heuristic algorithms, since use is always made of a randomizing factor to randomly check the points, the distribution movement toward the teacher, too, has the mentioned factor. In short, for any distribution point x_i , there is a relation as follows:

$$x_i^{new} = r_i(T_A - T_f x_i) \tag{1}$$

where r_i is a random number between 0 and 1, T_A is the coordinates of the teacher point, and T_f is the teacher training factor selected randomly to be either 1 or 2.

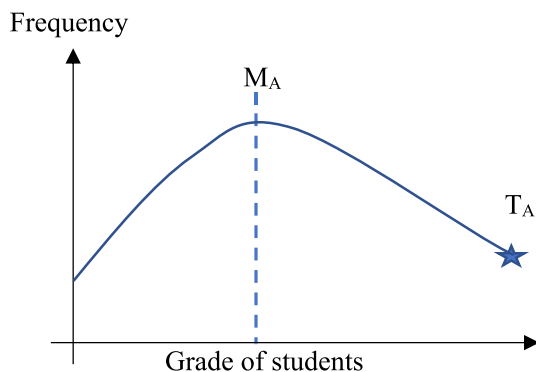


Fig. 2 Bell distribution of students grads

Now, if (x_i^{new}) has a higher value than x_i , it will replace it. Training step changes are shown in Fig. 3.

Learning stage

Next is the learning step where the mutual learning of the students of one class is simulated in such a way that for each student, another one is randomly selected. Then, if the second has a better position than the first as regards the objective function, the first will move toward the second; otherwise, the second will move toward the first.

This algorithm-diversifying move too has a random factor, and the step for each student is as follows:

$$x_i^{new} = \begin{cases} x_i^{old} - r_i(x_j - x_i) & \text{iff } (x_i) \geq f(x_j) \\ x_i^{old} + r_i(x_j - x_i) & \text{iff } (x_i) < f(x_j) \end{cases} \tag{2}$$

Next is the checking of algorithm termination conditions; if conditions are met, the algorithm terminates, and if not, the loop is repeated.

Meshless local Petrov–Galerkin (MLPG)

Used for the first time by Atluri and Zhu (1998) to solve potential equations (Atluri and Zhu 1998), MLPG (meshless local Petrov–Galerkin) has since been used by a large number of researchers in scientific and engineering problems. In this method, since the test and experiment functions are selected from two different spaces, many meshless methods have used it as a basis for their formulation (Akbari et al. 2010). It uses the moving least squares approximation function to construct the shape function, but as the latter does not satisfy the Delta Kronecker function conditions, it fails to apply the problem's necessary boundary conditions (Dirichlet Boundary Conditions) making the use of such other methods as the "collocation" and "penalty function" a necessity (Liu and Gu 2005). But since these methods add approximate values to the results, it would be better to replace with those that eliminate these approximations and bring the model

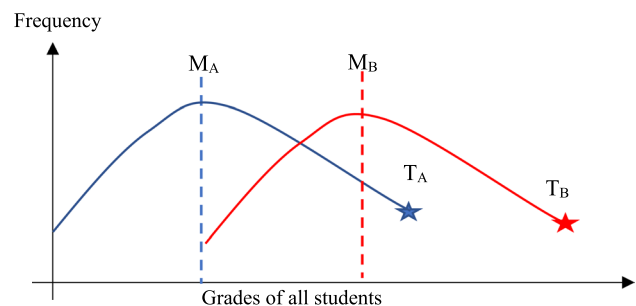


Fig. 3 Changes in grads at teaching stage

closer to reality. Although error rates are small in these methods, their removal and replacement with the moving Kriging method is a serious measure because by satisfying the Delta Kronecker function, it can apply the necessary boundary conditions without adding an approximation (Mohtashami et al. 2021). As it is necessary in this research to study and analyze the uncertainty of the problem's boundary conditions, the moving Kriging method is used to directly apply the necessary ones. According to different references, this method has been used since 2013 to do approximation and construct shape function in the field of solids; however, this is the first time it is being used in this study in the field of fluids, especially groundwater (Khankham et al. 2015).

Moving kriging

The moving Kriging approximation function is a well-known method for spatial interpolation in geometry and mining (Khankham et al. 2015). To formulate its shape function considers function $H(x)$ discretized by several nodes in domain Ω . There are x_i nodes, $i = 1, 2, \dots, N$ where N is the total number of nodes distributed in the domain, and it is assumed that only N nodes surrounding point x affect $H(x)$. Subdomain Ω_x that contains the surrounding nodes is called the approximation domain of point x , and since moving Kriging approximation $H^h(x)$ is defined at this point (Liu and Gu 2001), formulation of the shape function of the meshless moving Kriging is as follows:

$$H^h(x) = \sum_{i=1}^N \phi_i(x)H_i = \Phi(x)H, x \in \Omega_x \tag{3}$$

where $H = [H(x_1)H(x_2) \dots H(x_N)]^T$ is the function vector in domain Ω and $\Phi(x)$ is the shape function vector with size $1 \times N$ expressed as follows:

$$\Phi(x) = p^T(x)A + r^T(x)B \tag{4}$$

Matrices A and B are defined in Eqs. (4) and (5):

$$A = (P^T R^{-1} P)^{-1} P^T R^{-1} \tag{5}$$

$$B = R^{-1}(I - PA) \tag{6}$$

where I is an $N \times N$ unit matrix and vector $p(x)$ is as follows:

$$p^T(x) = [p_1(x)p_2(x) \dots p_N(x)] \tag{7}$$

In $N \times M$ matrix P , base polynomials are written for each point as follows:

$$P = \begin{bmatrix} p_1(x_1) & \dots & p_M(x_N) \\ \dots & \dots & \dots \\ p_1(x_N) & \dots & p_M(x_N) \end{bmatrix} \tag{8}$$

Matrix R and vector $r(x)$ are found as follows:

$$R = \begin{bmatrix} r(x_1, x_1) & \dots & r(x_1, x_N) \\ \dots & \dots & \dots \\ r(x_N, x_1) & \dots & r(x_N, x_N) \end{bmatrix} \tag{9}$$

$$r^T(x) = [r(x, x_1)r(x, x_2) \dots r(x, x_N)] \tag{10}$$

where $r(x_i, x_j)$ is a correlation function between two points located at X_i and X_j and represents the covariance of $H(x)$ real value:

$$r(x_i, x_j) = E[H(x_i)H(x_j)] \tag{11}$$

The above equations show that matrix R and $r(x_i, x_j)$ play important roles in the calculations. The simple correlation function, used frequently, is a Gaussian function (Mohtashami et al. 2021):

$$r(x_i, x_j) = e^{-\alpha_c \left(\frac{r_{ij}}{d_c}\right)^2} \tag{12}$$

where $r_{ij} = x_i - x_j$ and d_c and $\alpha_c > 0$ are constant-value correlation parameters used for fitting.

Governed equation of groundwater in unconfined aquifer

When the aquifer is unconfined, the governing equation in an unsteady state will be as follows based on Dupuit assumption and continuity equations (Dupuit 1863; Mays and Todd 2005):

$$\frac{\partial}{\partial x} \left(k_x H \frac{\partial H}{\partial x} \right) + \frac{\partial}{\partial y} \left(k_y H \frac{\partial H}{\partial y} \right) = \frac{S_y \partial H}{\partial t} + Q \times \delta(x - x_w)(y - y_w) + q \tag{13}$$

where H is the groundwater level (m), k is the hydraulic conductivity (m/day), s k_x is in the horizontal direction, k_y is in the vertical direction, S_y is dimensionless specific discharge, Q is concentrated discharge ($-$ ive if exploitation well and $+$ ive, m^3/day , if injection well), and q is the distributed flow ($+$ ive, e.g. rain or $-$ ive, e.g. evaporation) (Mohtashami et al. 2020). It is worth noting that since the equation is time-dependent (unsteady state), the initial conditions are derived from the steady state and then put in the equation (Mohtashami et al. 2019).

Objective function (OF)

In this study, the objective functions are defined as in Eqs. (14) and (15) borrowed from (Jafarzadeh and Khashei-Siuki (2018), Cieniawski et al. (1995):

$$E = (\text{abs}(h_{\text{Obs}} - h_{\text{Sim}})) \quad (14)$$

$$F = 1 - \exp(-E) \quad (15)$$

In Eq. (14), h_{Obs} and h_{Sim} are water levels observed in piezometers and simulated by the simulator model, respectively, E is estimation error, and F is the value of the objective function. The selected objective function varies in a 0–1 range and error $E > 2.3$ m will cause the objective function to tend to 1. Applying this objective function, especially for estimating the groundwater level, has caused the algorithm to search and discover the optimal points with very high severity.

The flowchart diagram of the MLPG-TLBO model is shown below (Fig. 4). The model, as mentioned in the introduction, has been formed by connecting two simulation and optimization models. The left part in the diagram shows the optimization section run at the main program of the simulation model. In the optimization diagram, the simulation model is executed after the parameters of the optimization model are given their initial values to calculate the objective function; then, the optimization steps continue after the initial values of the objective function are obtained (Table 1).

Results and discussion

To model the groundwater flow by the MLPG method, Birjand aquifer was first drawn by spreading points on its slope and boundary 500 m apart (Fig. 5) based on its earlier studies (Mohtashami et al. 2017) which enable the results obtained with this method to be compared with those of (Sadeghi tabas et al. 2016) and (Hamraz et al. 2015) based on the finite difference method. Next, the hydrodynamic information of each point was assigned to that node according to its position in the aquifer the hydrodynamic parameters of which include hydraulic conductivity and specific discharge information calibrated and validated by (Sadeghi tabas et al. 2016). The aquifer boundary conditions defined for the related points (shown by arrows in Fig. 1) are 0 for constant head and flow. It is worth mentioning that this model was calibrated and validated by Mohtashami et al. (2017) in both steady and unsteady modes the results of which are listed in Table 2; modeling period was one year with monthly time-steps.

As optimization requires the piezometers' observational values to be specified throughout the aquifer and for each time-step, they were interpolated with the ArcGIS software in each month and at the aquifer surface, and an observational value was assigned to each point in each time period. Then, the objective function was calculated based on these values and those obtained from the simulator model and checked, based on the minimum value of this function, to determine the best location for the piezometric well in the aquifer.

Table 2, the results of which were calibrated and validated based on the research of Mohtashami et al. (2017), compares errors of the MLPG model and those of the finite difference method.

The authors of this paper used the MLPG method proposed in previous studies to prepare, calibrate and validate the groundwater flow model of the Birjand aquifer. They had already calibrated the model in both steady and unsteady states and compared the results with those of the finite difference method (MODFLOW Package). The better and more accurate results of the meshless method were an evidence of the superiority of this model over the limited difference method due to its independence from the aquifer meshing which led to the elimination of the related errors. Results of these studies are presented in Table 2.

After coupling the meshless model to the optimization algorithm, the simulation–optimization calculations were done on a CORE I5/8 RAM/5200 U PC. This hybrid model was implemented 10 series the best of which was that of series 9 (with an objective function value = 0.132 m). The model implementation results are shown in Table 3.

Finally, the optimal location of the observational wells was selected based on series 9 implementation of the model. Piezometers' new positions are marked in blue in Fig. 6 where green indicates the previous locations of the observational wells in the aquifer.

As shown in the aquifer area, the optimal observational wells are located where extraction wells are less concentrated. While the spatial variations of wells 4, 6 and 9 are very high, those of 1, 2, 3, 5, 7 and 10 are almost as much as one node due to the proximity of observational wells to areas where the density of extraction wells is lower; this is quite checkable in well No. 4. New locations of observational wells are shown in Table 4 with their UTM coordinates.

The simulated and observed water levels in new observational wells are plotted on a graph and presented for piezometers 1, 4 and 7 in Fig. 7 to evaluate the performance of the optimization model to find the optimal location of the observational wells.

Water levels observed in new piezometers found by the meshless model and calculated by the finite difference method are compared in Fig. 7. In graphs of piezometers 1, 4, and 7 at their new locations in the aquifer, black, red and

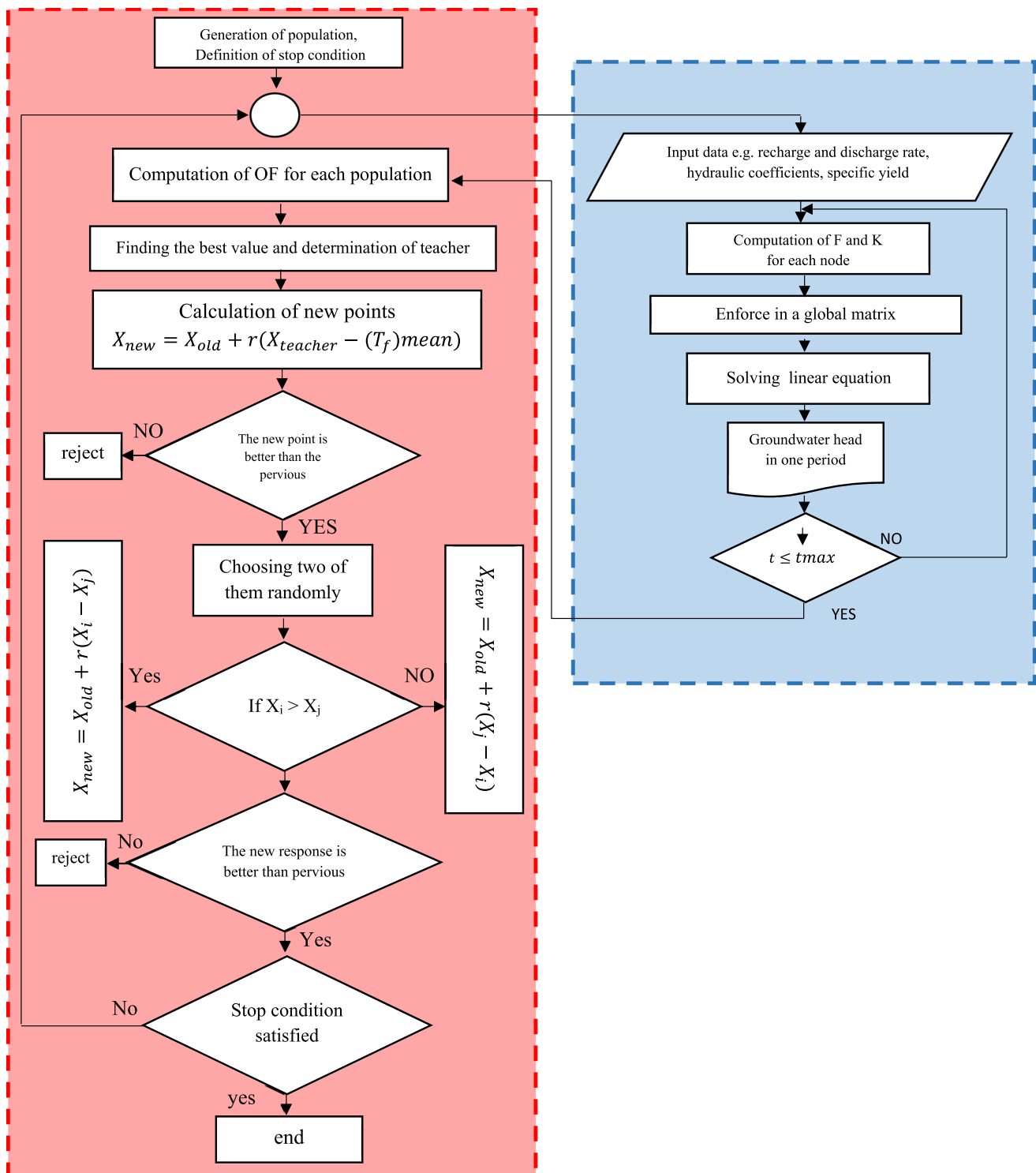


Fig. 4 Flowchart of MLPG-TLBO method

gray lines represent the water levels observed during modeling period, modeled by the meshless model and found by the finite difference method, respectively. In all diagrams, the meshless model yielded better and more accurate results than the finite difference method due to its independence

from the meshing of the solution domain. In Fig. 7a (piezometer 1), the meshless model and observational results do not differ much at the beginning of the period, but over time, the difference increases gradually and reaches 0.07 m in the last month; for the finite difference model, this difference is

Table 1 Coordinates of observation wells in Birjand aquifer

Well number	UTM <i>x</i>	UTM <i>y</i>	Well number	UTM <i>x</i>	UTM <i>y</i>
1	672076.92	3626500	6	681191.541	3638000
2	673616.684	3629000	7	693716.317	3641500
3	677358.12	3628000	8	696160.839	3639500
4	675,659.263	3634500	9	701775.426	3639000
5	674670.794	3638500	10	716167.142	3636000

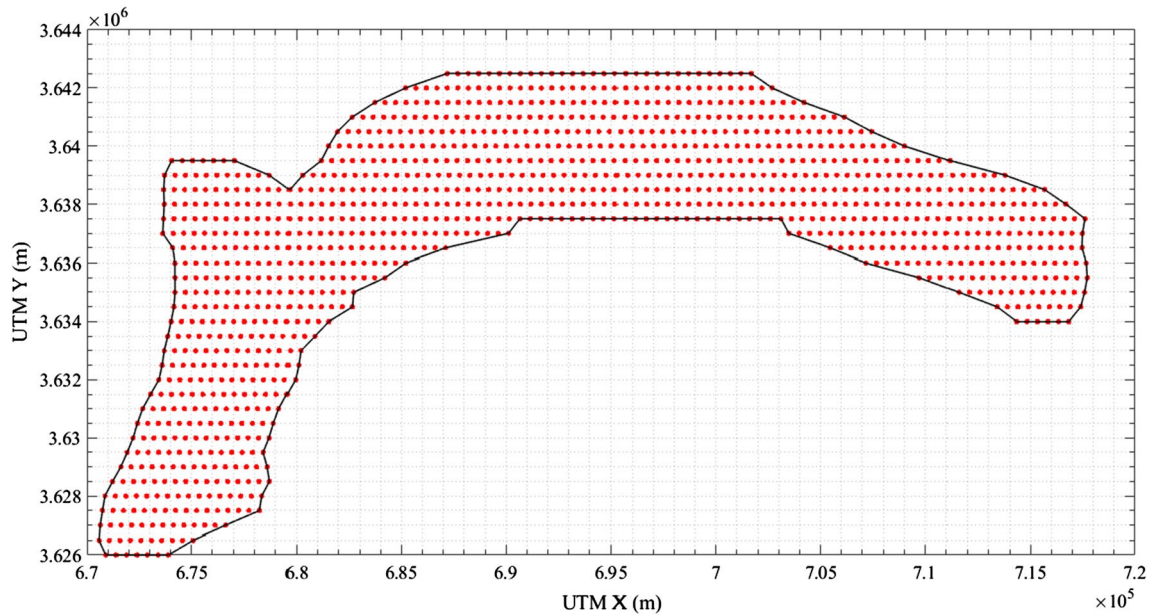


Fig. 5 Scattering nodes in Birjand aquifer

Table 2 Computation of error indices in unsteady state

Error criteria (<i>m</i>)	MLPG (Mohtashami et al. 2017)	FDM (Sadeghi Tabas et al. 2016)
Mean error	-0.08	0.159
Mean absolute error	0.573	1.434
Root mean square error	0.757	1.197

Table 3 The achieved results from MLPG-TLBO

Run number	Objective function (<i>m</i>)	Run number	Objective function (<i>m</i>)
1	0.159	6	0.155
2	0.161	7	0.148
3	0.153	8	0.152
4	0.184	9	0.132
5	0.169	10	0.136

0.11 m. In Fig. 7b, results of the meshless model are quite close to the observational data almost correlating until the month 6. Another point in 7b is the increase in the water level results of the finite difference method observable in periods 2 and 3 due to method-related errors. In Fig. 7c, unlike 7a, the meshless model is more accurate at the end of the period than at the beginning.

Figure 8 shows the regression coefficient of the results of the meshless and finite difference models where green dots represent the water level obtained from the meshless model in new piezometers and the orange dots show those of the finite difference model. As shown, the regression coefficient of the meshless model is higher than that of the finite difference model in all piezometers; the higher is this coefficient, the greater is the correlation between the model results and the observational data.

Finally, to evaluate the model accuracy, several known error criteria in the groundwater field were used and the mean error (ME), mean absolute error (MAE) and root mean square error (RMSE) indices were found for all piezometers (Table 5).

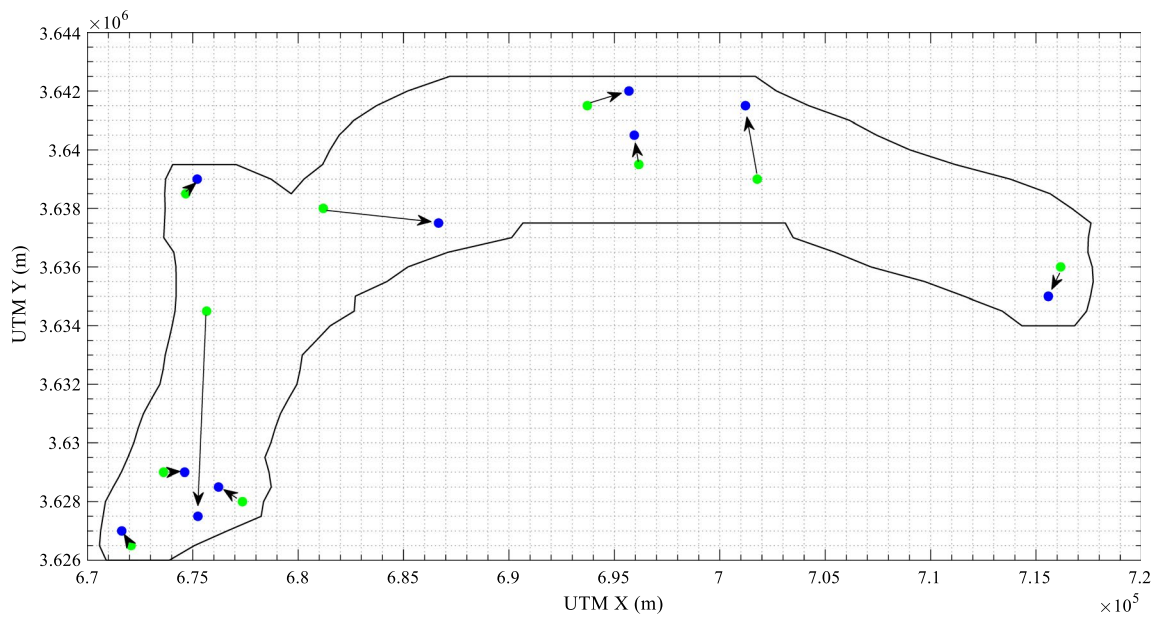


Fig. 6 The optimal location of observation wells

Table 4 Optimal coordinates of observation wells in Birjand aquifer

Well number	UTM x	UTM y	Well number	UTM x	UTM y
1	671632.311	3627000	6	686659.633	3637500
2	674116.684	3629000	7	695690.187	3642000
3	676724.451	3628500	8	695443.735	3640500
4	675245.214	3627500	9	701216.317	3641500
5	675211.756	3639000	10	715583.703	3635000

As shown, displacing piezometric wells to the optimal positions found by the MLPG-TLBO model reduced the RMSE by 0.423 m which is quite high and meaningful for such an aquifer volume and means the monitoring network designed to operate in this aquifer is suitable.

Conclusions

This study proposed a novel model, i.e. MLPG-TLBO, as a simulation–optimization method aiming at enhancing the accuracy of groundwater monitoring and determining the optimal locations for piezometers in Birjand aquifer. After coupling the teaching–learning-based optimization model to

the meshless flow model, already calibrated and validated in some studies, the optimal locations of ten piezometers were determined in Birjand aquifer and their observed water levels were compared with those found in different modeling periods computationally to evaluate the model performance proved to be acceptable because before applying the model, the RMSE was 0.757 m, but after optimization it reached 0.334 m. Considering the aquifer area, this difference is a huge volume of water the error of which was omitted by the MLPG-TLBO model. The acquired results also show the satisfactory performance of this model in this aquifer. It is noticeable that, in addition of giving a pervasive knowledge about groundwater behavior, this model helps the water engineers to define some scenarios for better management.

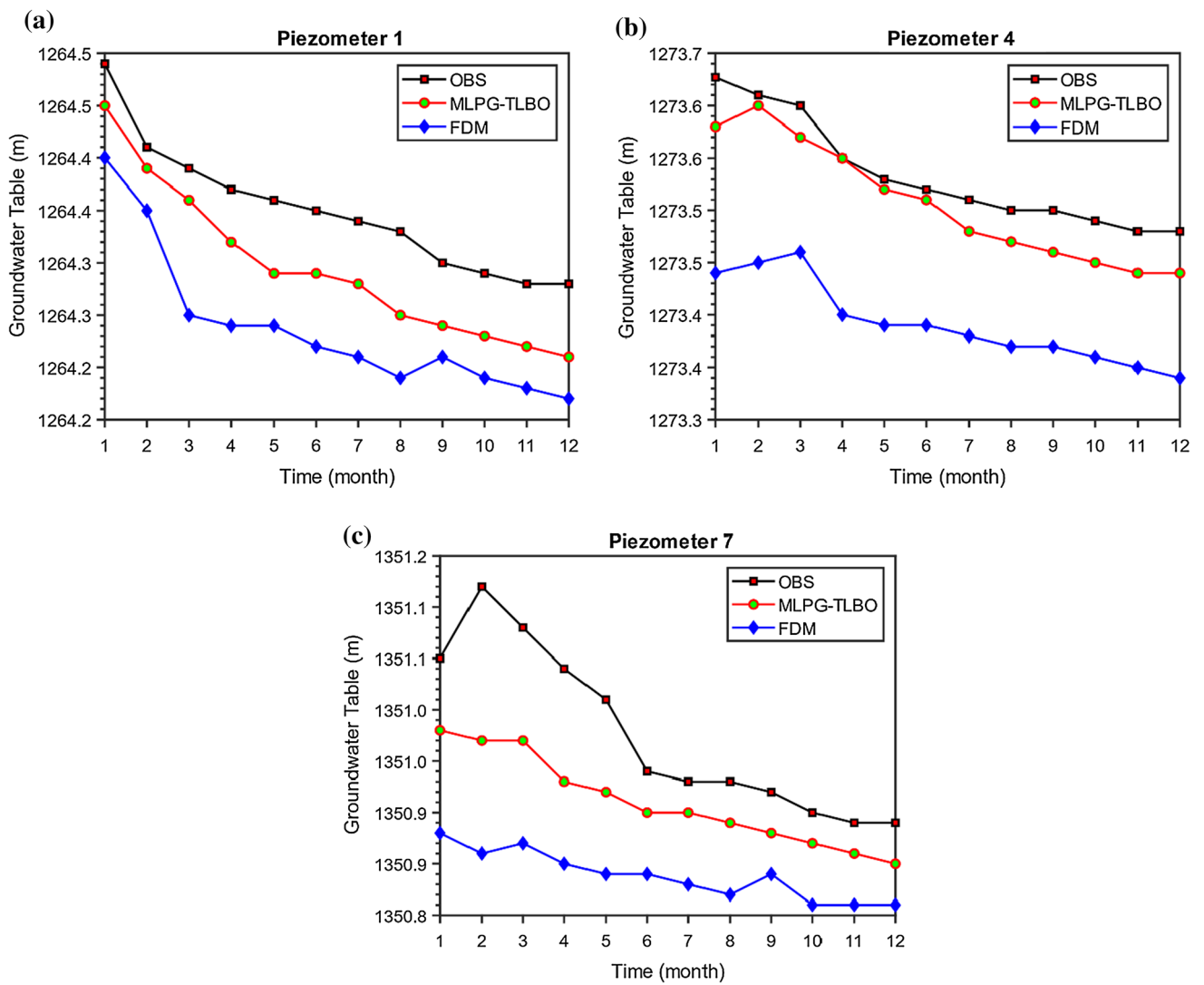


Fig. 7 Computation of groundwater head with MLPG-TLBO

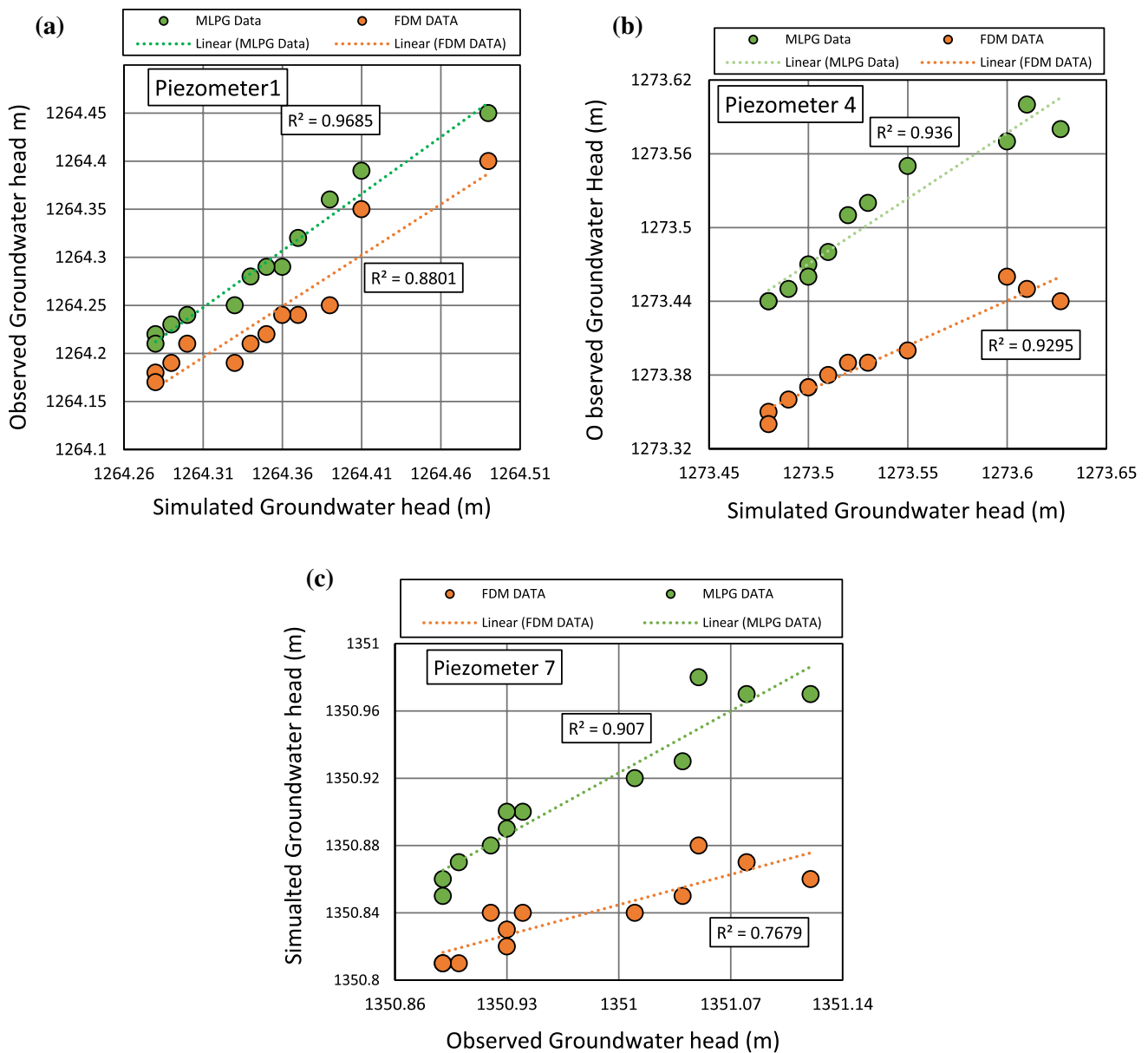


Fig. 8 Computation of regression coefficients for both MLPG-TLBO and FDM

Table 5 Computation of error indices in unsteady state for both MLPG-TLBO and FDM

Error criteria (<i>m</i>)	MLPG-TLBO	FDM (Khorshadizadeh et al. 2018)
Mean error	0.11	0.169
Mean absolute error	0.203	1.980
Root mean square error	0.334	1.483

Funding The author(s) received no specific funding for this work not applicable.

Data Availability The datasets used during the current study are available from the corresponding author on reasonable request.

Declarations

Conflict of interest The authors declare that they have no conflict of interest.

Consent for publication This manuscript also does not contain data from any individual person, and therefore, consent to publish is not applicable.

Ethics approval and consent to participate This manuscript does not report on or involve the use of any animal or human data or tissue.

Open Access This article is licensed under a Creative Commons Attribution 4.0 International License, which permits use, sharing, adaptation, distribution and reproduction in any medium or format, as long as you give appropriate credit to the original author(s) and the source, provide a link to the Creative Commons licence, and indicate if changes were made. The images or other third party material in this article are included in the article's Creative Commons licence, unless indicated otherwise in a credit line to the material. If material is not included in the article's Creative Commons licence and your intended use is not permitted by statutory regulation or exceeds the permitted use, you will need to obtain permission directly from the copyright holder. To view a copy of this licence, visit <http://creativecommons.org/licenses/by/4.0/>.

References

- Aboutalebi M, Bozorg-Haddad O, Loáiciga HA (2017) Multiobjective design of water-quality monitoring networks in river-reservoir systems. *J Environ Eng* 143(1):0401607
- Akbari R, Bagri A, Bordas SPA, Rabczuk T (2010) Analysis of thermoelastic waves in a two-dimensional functionally graded materials domain by the meshless local petrov-galerkin (MLPG) method. *Comput Model Eng Sci* 65(1):27–74
- Atluri S, Zhu TA (1998) A new MEshless method (MLPG) approach in computational mechanics. *Comput Mech*. <https://doi.org/10.1007/s004660050346>
- Cieniawski SE, Eheart JW, Ranjithan S (1995) Using genetic algorithm to solve a multi objective ground water monitoring problem. *Water Resour Res* 31:399–409
- Črepinšek M, Liu SH, Mernik L (2012) A note on teaching–learning-based optimization algorithm. *Inf Sci* 212(1):79–93
- Dhar, Patil RS (2012) Multiobjective design of groundwater monitoring network under epistemic uncertainty. *Water Resour Manag* 26(7):1809–1825
- Dupuit J (1863) *Estudes theoriques et pratiques sur le mouvement desEaux*. Dunod, Paris
- Hamraz S, Akbarpour A, Pourreza Bilondi M, Sadeghi Tabas S (2015) On the assessment of ground water parameter uncertainty over an arid aquifer. *Arab J Geosci* 8:10759–10773
- Jafarzadeh, Khashei-Siuki A (2018) Performance examination of optimization model of groundwater monitoring network based on gray wolf and neural network (GNM) (Case study: Birjand plain). *J Irrig Water Eng* 8(3):121–139
- Janatrostami S, Salahi A (2020) Designing an optimal groundwater quality monitoring network using a genetic algorithm-based optimization approach (case study: Guilan's aquifer). *Environ Sci* 18(2):19–40
- Khankham S, Luadsong A, Ascharyaphotha N (2015) MLPG method based on moving kriging interpolation for solving convection–diffusion equations with integral condition. *J King Saud Univ Sci* 27(4):292–301
- Khorashadizadeh M, Azizian G, Hashemi Monfared SA, Akbarpour A (2018) Sensitivity analysis of two-dimensional pollution transport model parameters in shallow water using RSA method. *Iran J Soil Water Res* 49(5):1119–1129
- Khorashadizadeh M, Hashemimonfared SA, Akbarpour A, Pourrezabilondi M (2016) Uncertainty assessment of pollution transport model using GLUE method. *Iran J Irrig Drainage* 10(3):284–293
- Khorashadizadeh M, Azizyan G, Hashemi Monfared SA, Akbarpour A, Shabani A (2020) A timetable and spatial planning for pollutant entrance to the river. *Int J Environ Sci Technol* 17(10):4171–4188
- Khorramdel NG, Keykhaei F (2016) Optimal design of observation wells in a groundwater monitoring network using meta-heuridtic genetic algorithm. *J Watershed Manag Res* 7(14):159–166
- Kollat JB, Reed PM, Maxwell RM (2011) Many-objective groundwater monitoring network design using bias-aware ensemble Kalman filtering, evolutionary optimization, and visual analytics. *Water Resour Res*. <https://doi.org/10.1029/2010WR009194>
- Liu GR, Gu YT (2001) A point interpolation method for two-dimensional solid. *Int J Numer Methods Eng* 50:937–951
- Liu GR, Gu YT (2005) *An introduction to meshfree methods and their programming*. Springer, Singapore
- Loaiciga HA, Charbeneau RJ, Everett LG, Fogg GE, Hobbs BF, Rouhani S (1992) Review of ground-water quality monitoring network design. *J Hydraul Eng* 118(1):11–37
- Majidi Khalilabad N, Mohtashami A, Akbarpour A (2021) Determination of well's capture zones using random walk algorithm and feflow simulation model. *Iran J Irrig Drain* 14(6):1984–2002
- Mirzaei-Nodoushan F, Bozorg Haddad O, Khayyat Kholghi M (2016) Two-objective design of groundwater-level monitoring network using NSGA-II in Eshtehard Plain. *Iran J Soil Water Res* 47(2):345–354
- Mirzaei-Nodoushan F, Bozorg Haddad O, Khayat Kholghi M (2019) Optimization and development of groundwater-level monitoring network in Eshtehard Plain. *Watershed Eng Manag* 11(1):273–283
- Mishara K, Coulibaly P (2009) Developments in hydrometric network design: a review. *Rev Geophys*. <https://doi.org/10.1029/2007RG000243>
- Mohtashami A, Akbarpour A, Mollazadeh M (2017) Development of two dimensional groundwater flow simulation model using meshless method based on MLS approximation function in unconfined aquifer in transient state. *J Hydroinform* 19(5):640–652
- Mohatshami A, Hashemi Monfared SA, Azizyan G, Akbarpour A (2019) Prediction of groundwater fluctuations using meshless local Petrov-Galerkin numerical method in a field aquifer (Birjand aquifer). *Int J Numer Methods Civil Eng* 3(4):33–41
- Mohtashami A, Hashemi Monfared SA, Azizyan G, Akbarpour A (2020) Determination of the optimal location of wells in aquifers with an accurate simulation-optimization model based on the meshless local Petrov-Galerkin. *Arabian J Geosci* 13(2):1–13
- Mohtashami A, Hashemin Monfared SA, Azizyan G, Akbarpour A (2021) Estimation of Parameters in groundwater modeling by particle filter linked to the meshless local Petrov-Galerkin numerical method. *J Hydraul Struct* 7(1):16–37
- Mohtashami A, Hashemi Monfared SA, Azizyan G, Akbarpour A (2022) Application of meshless local petrov-Galerkin approach for steady state groundwater flow modeling. *Water Supply*. <https://doi.org/10.2166/ws.2022.015>
- Rao RV, Savsani VJ, Vakharia DP (2011) Teaching–learning-based optimization: a novel method for constrained mechanical design optimization problems. *Comput Aided Des* 43(3):303–315
- Rao RV, Savsani VJ, Vakharia DP (2012) Teaching–learning-based optimization: an optimization method for continuous non-linear large scale problems. *Inf Sci* 183(1):1–15
- Sadeghi tabas S, Samadi SZ, Akbarpour A, Pourreza Bilondi M (2016) Sustainable groundwater modeling using single-and multi-objective optimization algorithms. *Journal of Hydroinform* 18(5):1–18
- Temur R (2021) Optimum design of cantilever retaining walls under seismic loads using a hybrid TLBO algorithm. *Geomech Eng* 24(3):237–251
- Mays LW, Todd DK (2005) *Groundwater Hydrology*. John Wily and Sons, Inc., Arizona State University, Third addition
- Veladi H, Beigi Zali R (2021) Optimum design of single-layer dome structures using a hybrid charged system search and teachinglearning-based optimization. *Int J Optim Civil Eng* 119(3):497–513

Publisher's Note Springer Nature remains neutral with regard to jurisdictional claims in published maps and institutional affiliations.